# Supplementary Information

# Interfacial chemistry at solid-liquid van der Waals heterojunctions enabling sub-5 nm Ohmic contacts for monolayer semiconductors

Dexing Liu, Shengdong Zhang and Min Zhang[1*]

School of Electronic and Computer Engineering, Peking University, Shenzhen 518055, China.

Supplementary Figures S1-9

Supplementary Table S1

---

[1*] Corresponding author.
E-mail address: zhangm@ece.pku.edu.cn (M. Zhang).

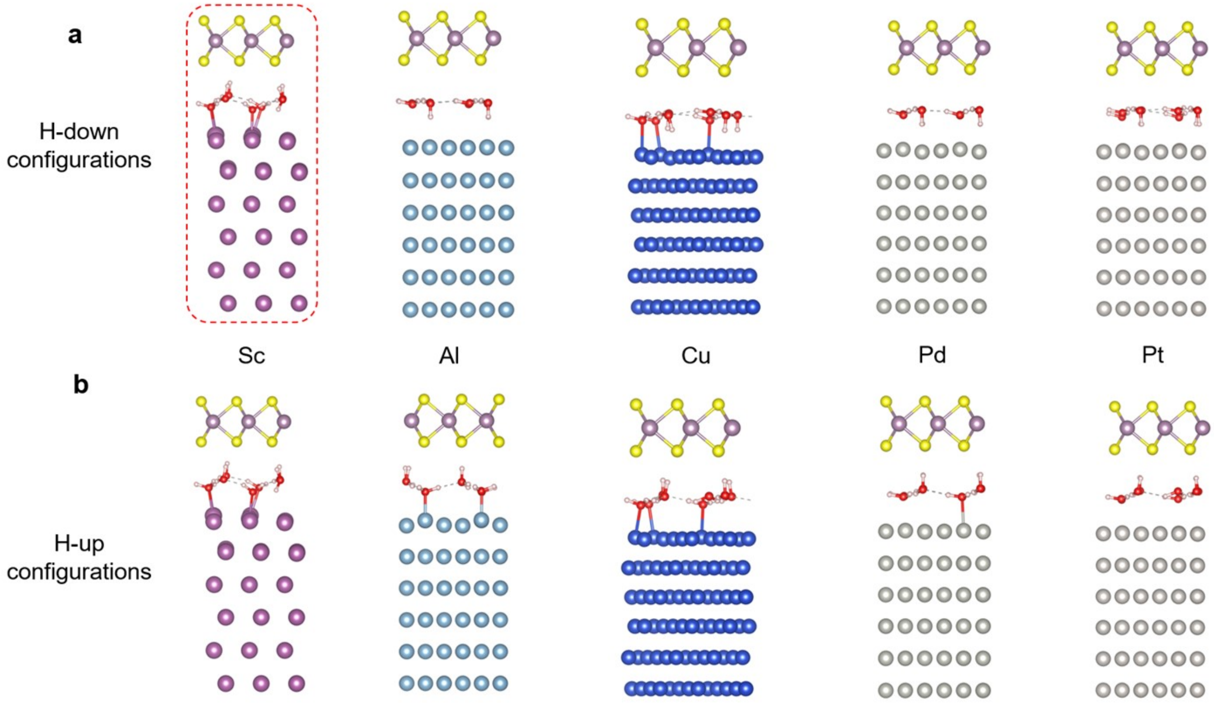

**Figure S1. Relaxed geometrical structures of ice-like bilayer water intercalated metal/MoS$_2$ vdW heterojunctions with H-down (a) and H-up (b) configurations.** The H-down and H-up configurations are recognized by the orientation of the hydrogen atom in the second water molecule towards and away from the metal surface, respectively. When the metal is scandium (Sc), the structure after relaxation is always the H-up configuration (circled in red dashed lines), regardless of whether the initial configuration is H-down or H-up.

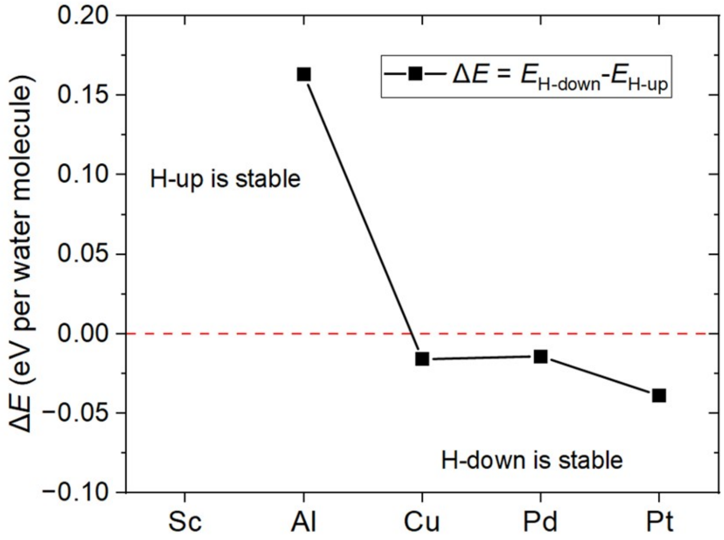

**Figure S2. Energy difference between H-down configuration and H-up configuration for different metal/$H_2O/MoS_2$ heterojunctions.** The missing data for metal as Sc is due to the Sc/$H_2O/MoS_2$ heterojunction with H-down configuration being energetically unstable. For heterojunctions where the metals are Sc and Al, the water intercalation system in the H-up configuration is stable, whereas for heterojunctions where the metals are Cu, Pd and Pt, the water intercalation system in the H-down configuration is stable.

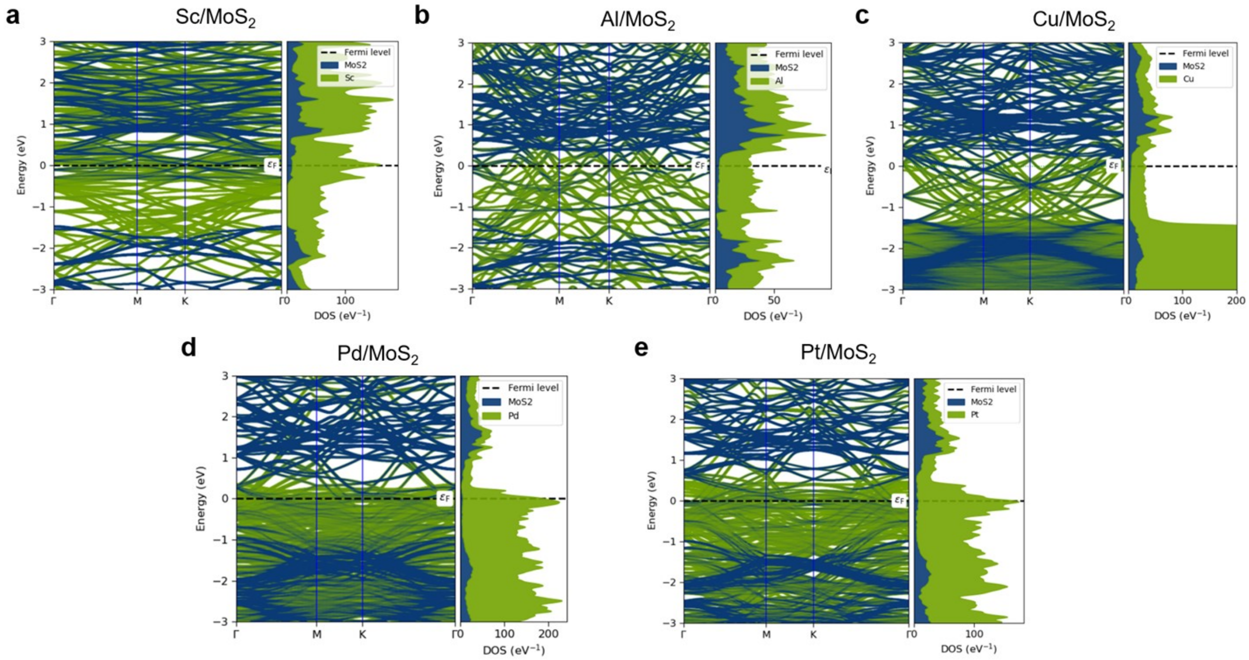

**Figure S3. Electronic properties of various metal/MoS$_2$ heterojunctions.** Projected band structures (left panel) and projected density of states (right panel) for Sc/MoS$_2$ (a), Al/MoS$_2$ (b), Cu/MoS$_2$ (a), Pd/MoS$_2$ (a), and Pt/MoS$_2$ heterojunctions. Green represents the contribution of metal, and blue represents the contribution of MoS$_2$. The Fermi-level, shown by the black dashed line, is set to zero. Significant metal-induced interfacial states and Fermi-level pinning effects are observed in all systems due to the strong orbital hybridization between the metal and MoS$_2$.

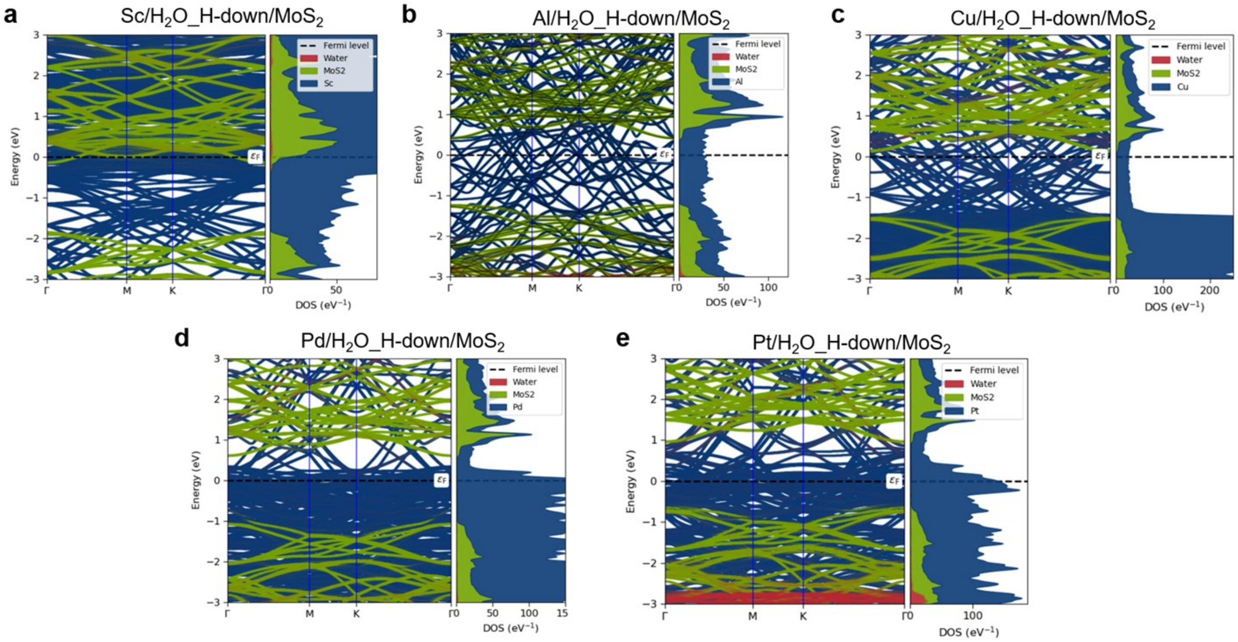

**Figure S4. Electronic properties of various ice-like bilayer water intercalated metal/$MoS_2$ heterojunctions with H-down configurations.** Projected band structures (left panel) and projected density of states (right panel) for Sc/$H_2O$_H-down/$MoS_2$ (a), Al/$H_2O$_H-down/$MoS_2$ (b), Cu/$H_2O$_H-down/$MoS_2$ (a), Pd/$H_2O$_H-down/$MoS_2$ (a), and Pt/$H_2O$_H-down/$MoS_2$ heterojunctions. Green represents the contribution of $MoS_2$, red represents the contribution of water, and blue represents the contribution of metal. The Fermi-level, shown by the black dashed line, is set to zero.

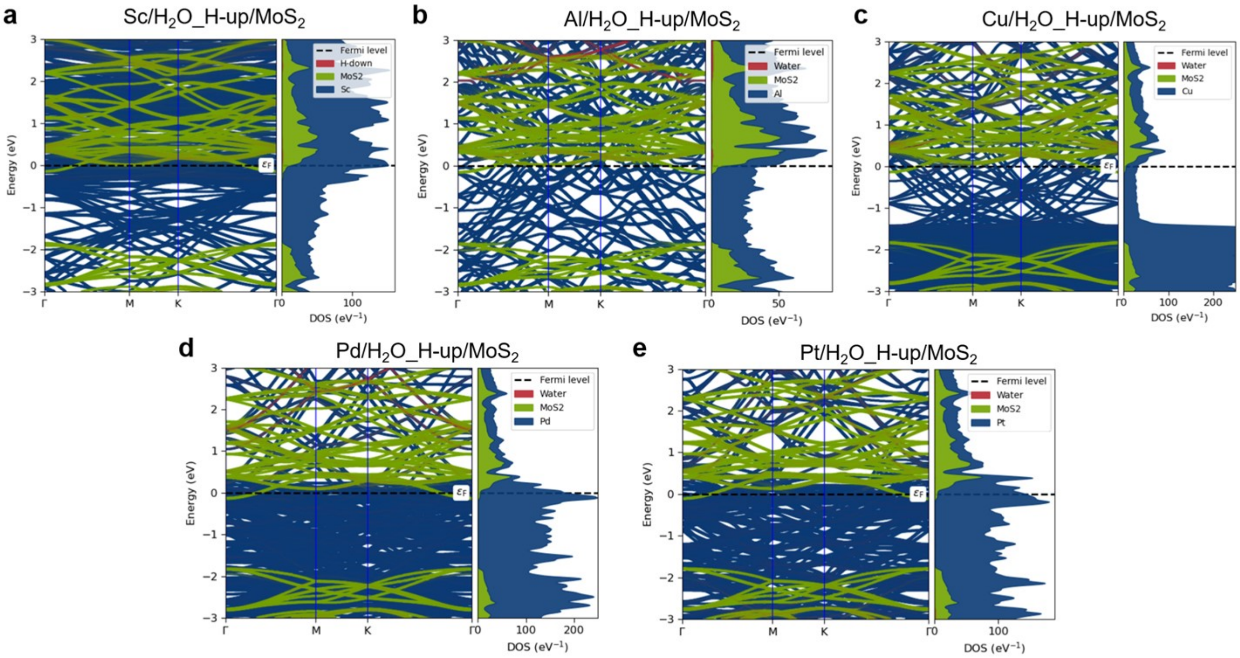

**Figure S5. Electronic properties of various ice-like bilayer water intercalated metal/MoS$_2$ heterojunctions with H-up configurations.** Projected band structures (left panel) and projected density of states (right panel) for Sc/H$_2$O_H-up/MoS$_2$ (a), Al/H$_2$O_H-up/MoS$_2$ (b), Cu/H$_2$O_H-up/MoS$_2$ (a), Pd/H$_2$O_H-up/MoS$_2$ (a), and Pt/H$_2$O_H-up/MoS$_2$ heterojunctions. Green represents the contribution of MoS$_2$, red represents the contribution of water, and blue represents the contribution of metal. The Fermi-level, shown by the black dashed line, is set to zero.

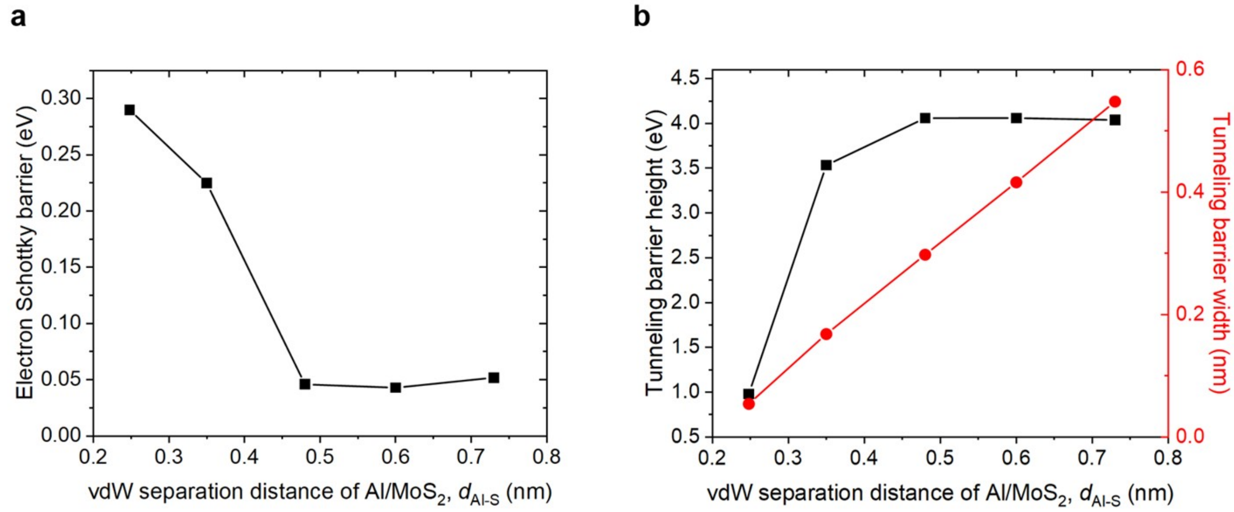

**Figure S6. The trade-off between the tunneling barriers and Schottky barriers in Al/MoS$_2$ vdW heterojunctions.** (a) Electron Schottky barrier as a function of vdW separation distance in Al/MoS$_2$ vdW heterojunctions. (b) Tunneling barrier height (black) and width (red) as a function of vdW separation distance in Al/MoS$_2$ vdW heterojunctions.

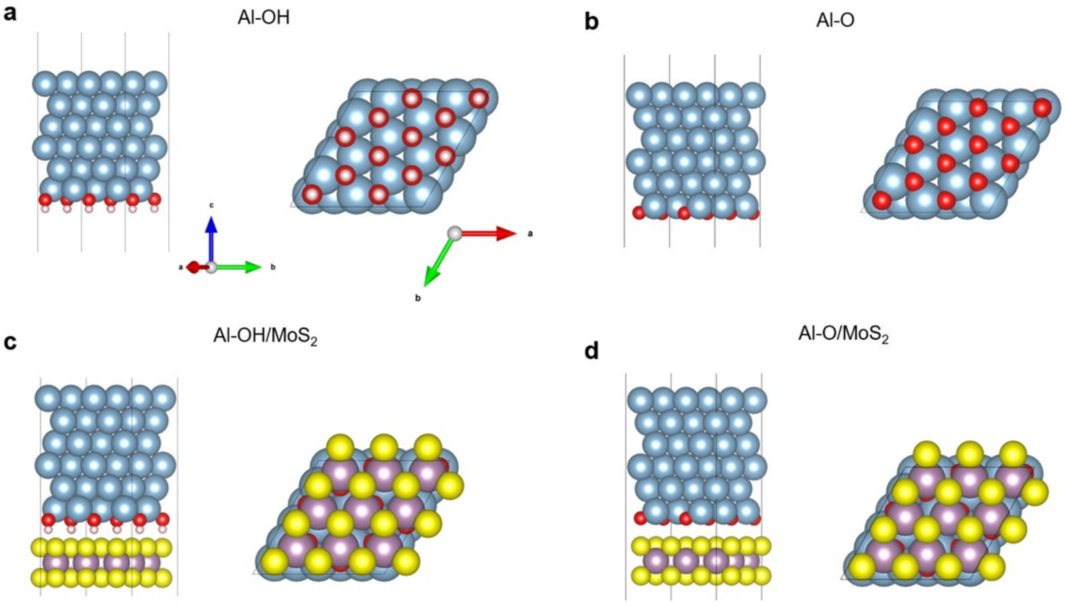

**Figure S7. Relaxed geometrical structures of (a) OH-covered Al (111) surface, (b) O-covered Al (111) surface, (c) OH-covered Al (111)/MoS$_2$ heterojunction, and (d) O-covered Al (111)/MoS$_2$ heterojunction.**

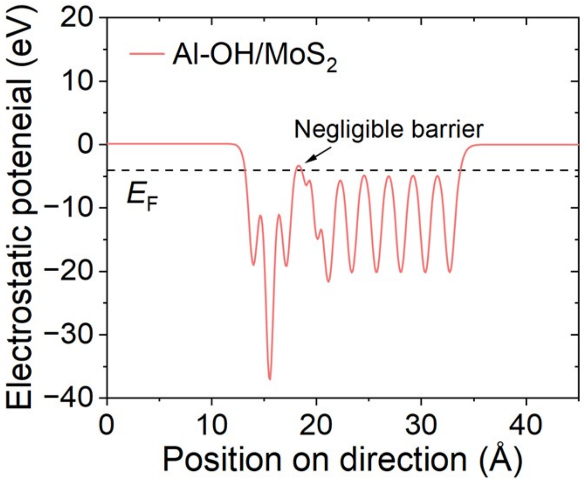

**Figure S8. Plane-averaged electrostatic potential along the surface-normal *z*-direction of OH-covered Al (111)/MoS$_2$ heterojunction.** The Fermi-level is shown by the black dashed line.

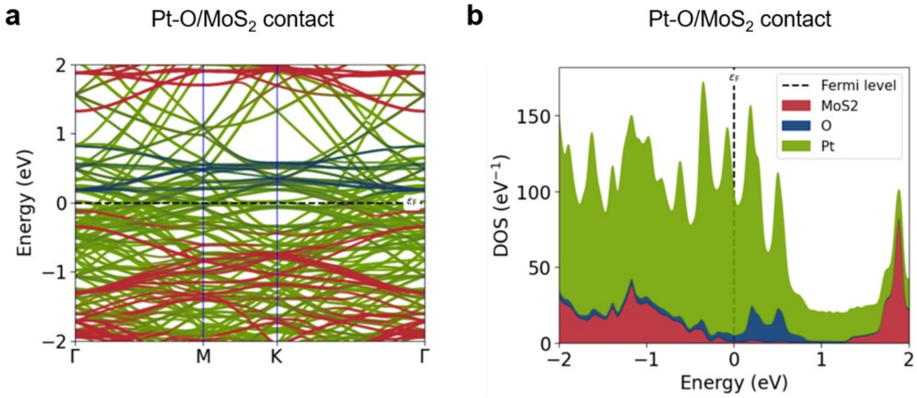

**Figure S9. Electronic properties of O-covered Pt/MoS$_2$ heterojunction.** (a) Projected band structures. (b) Projected density of states. The Fermi-level, shown by the black dashed line, is set to zero.

## Supplementary Table

**Table S1. Separation spacing between metal and semiconductor ($d_{M-S}$), binding energies ($E_b$), and adsorption energies ($E_{ad}$) of adsorbed structures of ice-like water bilayer between monolayer $MoS_2$ and clean metal surfaces.**

| Configurations ($M/H_2O/MoS_2$) | $d_{M-S}$ (Å) | $E_b$ (meV $Å^{-2}$) |  | $E_{ad}$ (kJ $mol^{-1}$) | $E_{H\,bond}$ (kJ $mol^{-1}$) | $E_{ad}-E_{H\,bond}$ (kJ $mol^{-1}$) |
|---|---|---|---|---|---|---|
|  |  | $E_{bM}$ | $E_{bS}$ |  |  |  |
| H_up configurations |  |  |  |  |  |  |
| Sc (0001) | 6.00 | -90.43 | -43.27 | **-120.22** | -26.60 | -93.62 |
| Al (111) | 5.97 | -60.48 | -44.55 | **-101.81** | -38.32 | -63.49 |
| Cu (111) | 5.85 | -48.69 | -31.62 | -99.47 | -42.74 | -56.73 |
| Pd (111) | 6.07 | -41.96 | -27.90 | -96.27 | -45.33 | -50.94 |
| Pt (111) | 6.21 | -42.31 | -24.49 | -95.73 | -45.24 | -50.49 |
| H_down configurations |  |  |  |  |  |  |
| Al (111) | 6.33 | -29.68 | -19.71 | -86.06 | -47.06 | -39.00 |
| Cu (111) | 5.69 | -52.79 | -22.58 | **-101.00** | -42.49 | -58.51 |
| Pd (111) | 5.90 | -48.16 | -20.55 | **-97.64** | -43.17 | -54.47 |
| Pt (111) | 5.97 | -50.93 | -21.12 | **-99.47** | -42.79 | -56.68 |
| OH- or O-covered metal surfaces |  |  |  |  |  |  |
| Al-OH (111) | 1.87 | -94.30 |  | - | - | - |
| Al-O (111) | 2.93 | -46.70 |  | - | - | - |
| Pt-O (111) | 2.67 | -46.35 |  | - | - | - |
| Direct contacts without water |  |  |  |  |  |  |
| Sc (0001) | 2.56 | -141.69 |  | - | - | - |
| Al (111) | 2.48 | -86.57 |  | - | - | - |
| Cu (111) | 2.07 | -142.60 |  | - | - | - |
| Pd (111) | 2.22 | -162.35 |  | - | - | - |
| Pt (111) | 2.31 | -126.06 |  | - | - | - |

Here the $E_b$ is defined as:

$$E_b = (E_{M/S} - E_M - E_S)/A,$$

where $E_{M/S}$, $E_M$, and $E_S$ represent the total energies of the M/S junction, the metal layer in the junction, and the semiconductor layer in the junction, respectively. $A$ is the area of the junction, which is 78.91 Å$^2$. In configurations with intercalated water, $E_b$ can be divided into two parts, $E_{bM}$ and $E_{bS}$, representing the binding energy between the water-covered semiconductor and the metal, and between the semiconductor and the water-covered metal, respectively. The average adsorption energies ($E_{ad}$) are calculated from the following expression:

$$E_{ad} = (E_{M/H_2O/S} - E_M' - E_S' - NE_{H_2O})/N,$$

where $E_{M/H_2O/S}$ is the total energy of adsorbed system, $E_M'$ is the energy of the optimized clean metal, $E_S'$ is the energy of the optimized clean semiconductor, $E_{H_2O}$ is the energy of an isolated $H_2O$ molecule, and $N$ is the number of $H_2O$ molecules. The total adsorption energy $E_{ad}$ can be decomposed into the sum of the hydrogen-bonding energy between water molecules ($E_{H\,bond}$) and the interaction energy between adsorbates and substrates ($E_{ad} - E_{H\,bond}$). $E_{H\,bond}$ can be estimated from the following expression:

$$E_{H\,bond} = (E_{NH_2O} - NE_{H_2O})/N,$$

where $E_{NH_2O}$ is the total energy of adsorbed water molecules in the adsorbed system.